Inorg. Chem. **2003**, *42*, 605–611

Tuning the Properties of the Osmium Nitrido Group in $TpOs(N)X_2$ by Changing the Ancillary Ligand

Ahmad Dehestani, Werner Kaminsky,[†] and James M. Mayer*

Department of Chemistry, University of Washington, Box 351700, Seattle, Washington 98195-1700

Received September 11, 2002

$TpOs(N)(OAc)_2$ (**2**) is formed upon reaction of $TpOs(N)Cl_2$ (**1**) with excess silver acetate (Tp = hydrotrispyrazolylborate). Treatment of **2** with protic acids HX gives the osmium(VI) complexes $TpOs(N)X_2$, where X = trifluoroacetate (TFA, **3**), trichloroacetate (TCA, **4**), tribromoacetate (TBA, **5**), bromide (**6**), oxalate ($X_2 = O_2C_2O_2$, **7**), or nitrate (ONO_2, **8**). Cyclic voltammetry studies of **1**–**8** show irreversible reductions of Os^{VI} to Os^{V}, varying over a range of 0.63 V. Much smaller relative variations are observed in ^{15}N NMR chemical shifts, $\nu(Os{\equiv}N)$ stretching frequencies, and optical absorbances. Compounds **1**–**8** all react with PPh_3 by nucleophilic attack at the nitride ligand, yielding $TpOs(NPPh_3)X_2$. The reactions are accelerated by more electron withdrawing ligands X. The relative rates correlate with the peak reduction potentials although the effect is small: the rates vary by only 10^2 while the 0.63 V change in $E_{p,c}$ corresponds to a change in equilibrium constant for electron transfer of $\sim 10^{11}$. Compounds **1**–**8** also react with triphenylboron, BPh_3, with formation of borylanilido complexes $TpOs[N(Ph)BPh_2]X_2$. However, rate constants for reactions with BPh_3 to yield Os^{IV} boryl–amido complexes do not in general correlate with one-electron-reduction potentials. This is likely due to the mechanism of the BPh_3 reactions being a two-step process and not simply nucleophilic attack.

Introduction

Multiply bonded ligands, such as nitrido or oxo groups, can react as electrophiles or nucleophiles. When they react as electrophiles, the net result is usually two-electron reduction of the metal center and formation of new chemical bond(s) (eq 1). This coupling of redox activity and bond

$$L_nM^{n+}(X) + :Nu \rightarrow L_nM^{(n-2)+}(X{-}Nu) \qquad (1)$$

formation and the resulting penchant for two-electron reactivity are among the reasons that such compounds are so valuable as oxidants for organic compounds. A variety of osmium(VI) nitrido compounds are known,[1] and the nitrido ligand can react as either an electrophile or a nucleophile depending on the ligand environment. For example, the nitride ligands of $[Os^{VI}(N)X_4]^-$ (X = Cl or Br) are electrophilic and subject to nucleophilic attack by phosphines (PAr_3) to afford the phosphiniminato complexes $Os(NPR_3)X_3(PAr_3)_2$.[2] In contrast, the nitride ligands of the related tetraalkyl and 1,2-benzenedithiolate derivatives $[Os(N)R_4]^-$ and $[Os(N)(bdt)_2]^-$ are electron rich and readily add R^+ to make imido compounds, due to electron-releasing alkyl and thiolate ligands.[3,4]

We have previously described a number of reactions in which $TpOs^{VI}(N)Cl_2$ (**1**) acts as an electrophile at the nitrido ligand [Tp = hydrotris(pyrazolyl)borate].[5,6] For instance, **1** reacts rapidly with triphenylphosphine to give the phosphiniminato complex $TpOs^{IV}(NPPh_3)Cl_2$.[6] Triphenylboron undergoes an unusual reaction with **1** to afford the borylanilido compound $[TpOs^{IV}\{N(Ph)BPh_2\}Cl_2]$ (eq 2).[5] This is an example of C−N bond formation by carbanion addition to the nitrido ligand.[5b]

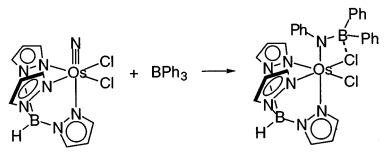

(2)

This report describes a systematic study of how changing the chlorides to other ancillary ligands affects the reactivity,

* Author to whom correspondence should be addressed. E-mail: mayer@chem.washington.edu.

[†] UW crystallography facility.

(1) Griffith, W. P. *Coord. Chem. Rev.* **1972**, *8*, 369.
(2) Griffith, W. P.; Pawson, D. *J. Chem. Soc., Dalton Trans.* **1973**, 531.
(3) Marshman, R. W.; Shapley, P. A. *J. Am. Chem. Soc.* **1990**, *112*, 8369.
(4) Sellman, D.; Wemple, M. W.; Donaubawer, W.; Heinemann, F. W. *Inorg. Chem.* **1997**, *36*, 1379.

10.1021/ic0260264 CCC: $25.00
Published on Web 12/28/2002

Scheme 1

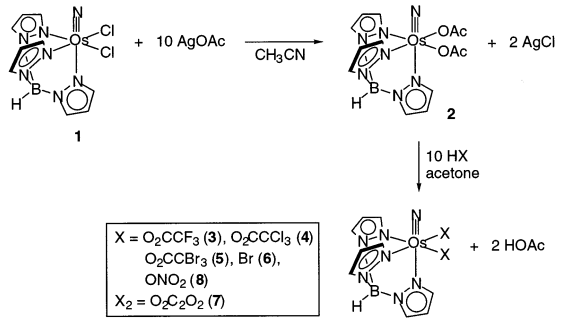

spectroscopic, electrochemical, and structural properties of $TpOs(N)X_2$ compounds. A key theme of this work is to explore the relationship between bond-forming reactivity and one-electron redox properties, in this case measured by cyclic voltammetry. The oxidizing power of reagents is often quantified by electrochemical potentials, but these do not simply relate to the inner-sphere multielectron processes typical of metal−ligand multiple bonds such as those shown in eqs 1 and 2.

Results

Syntheses and Structures of $TpOs(N)X_2$. $TpOs(N)(OAc)_2$ (**2**) is prepared by refluxing excess silver acetate with $TpOs(N)Cl_2$ (**1**) in acetonitrile for 12 h. Column chromatography on silica gel affords pure **2** in 70−90% yield. Related silver metatheses were unsuccessful for AgF and AgOTf (OTf = triflate, OSO_2CF_3). Complex **2** is a valuable precursor for the preparation of other substituted $TpOs(N)X_2$ complexes. Treatment of acetone solutions of **2** with an excess of the corresponding acid, HX, yields the air stable compounds $TpOs(N)(TFA)_2$ (**3**, TFA = trifluoroacetate), $TpOs(N)(TCA)_2$ (**4**, TCA = trichloroacetate), $TpOs(N)(TBA)_2$ (**5**, TBA = tribromoacetate), $TpOs(N)Br_2$ (**6**), $TpOs(N)(O_2C_2O_2)$ (**7**, $O_2C_2O_2$ = oxalate), and $TpOs(N)(ONO_2)_2$ (**8**). The synthetic approach is depicted in Scheme 1. The related fluoride complex could be generated (and the triflate derivative from the fluoride complex plus MeOTf), but these could not be obtained in pure form and were only characterized by ^{1}H NMR and mass spectrometry.

Single-crystal X-ray structures have been solved for the trifluoroacetate and nitrate complexes **3** and **8**. Crystal refinement data are given in Table 1, and selected bond lengths and angles are given in Table 2. ORTEP diagrams are displayed in Figures 1 and 2. The structures are similar to each other and to other Tp and nitrido complexes.[5−7] The typically short Os≡N triple bonds push the cis ligands away [all N(7)−Os−X angles are >90°] and exerts a strong trans influence.[8] The geometric features of the Tp ligand also contribute to the distorted octahedral structures, with N_{pz}−Os−N_{pz} angles less than 90°. As noted by Chang et al. and confirmed here, M≡N bond distances in $[Os^{VI}(N)L]$ do not vary with the electron-donating properties of L.[9]

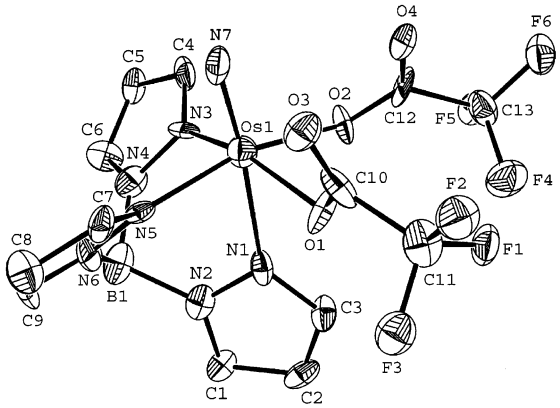

Figure 1. ORTEP drawing of $TpOs(N)(TFA)_2$ (**3**).

Table 1. Crystal and Structural Refinement Data[a]

	$TpOs(N)TFA_2$ (**3**)	$TpOs(N)(ONO_2)_2$ (**8**)
empirical formula	$C_{13}H_{10}BF_6N_7O_4Os$	$C_9H_{10}BN_9O_6Os$
fw	643.29	541.27
cryst syst	monoclinic	monoclinic
cryst size (mm)	0.25 × 0.10 × 0.05	0.24 × 0.05 × 0.005
space group	$P2_1/c$ (No. 13)	$P2_1/n$ (No. 14)
unit cell (Å, deg)		
a	17.608(2)	7.264(8)
b	13.718(4)	13.237(11)
c	19.390(4)	16.43(2)
α	90	90
β	156.47(2)	93.26(5)
γ	90	90
vol (Å^3)	1870.2(7)	1578(3)
Z	4	4
density (g/cm^3, calcd)	2.285	2.279
abs coeff (mm^{-1})	6.917	8.135
temp (K)	130(2)	130(2)
reflns collected	4786	4026
indep reflns	1869	2174
no. of params	289	235
final *R*, R_w (%)	6.41, 16.42	6.25, 13.41
GOF	1.042	0.852

[a] The radiation for both structures was Mo Kα (λ = 0.71073 Å).

Table 2. Selected Bond Lengths (Å) and Angles (deg) for $TpOs(N)(TFA)_2$ (**3**) and $TpOs(N)(ONO_2)_2$ (**8**)

	$TpOs(N)(TFA)_2$ (**3**)	$TpOs(N)(ONO_2)_2$ (**8**)
Os(1)−N(1)	2.289(20)	2.219(19)
Os(1)−N(3)	2.024(19)	2.045(16)
Os(1)−N(5)	2.044(16)	2.091(16)
Os(1)−O(1)	2.030(17)	2.009(14)
Os(1)−O(2)	1.996(14)	2.019(14)
Os(1)≡N(7)	1.602(20)	1.654(17)
N(3)−Os(1)−N(1)	80.63(6)	80.93(7)
N(5)−Os(1)−N(1)	82.84(6)	81.41(7)
N(3)−Os(1)−N(5)	89.93(8)	88.25(7)
N(1)−Os(1)−N(7)	174.16(8)	174.34(7)
N(3)−Os(1)−N(7)	95.38(8)	96.36(7)
N(5)−Os(1)−N(7)	92.9(8)	93.57(7)
O(1)−Os(1)−N(3)	159.20(7)	161.66(7)
O(2)−Os(1)−N(5)	164.55(6)	160.23(7)
O(1)−Os(1)−N(5)	92.55(7)	86.78(6)
O(2)−Os(1)−N(3)	89.71(7)	94.11(6)
O(1)−Os(1)−N(1)	79.20(7)	80.87(6)
O(2)−Os(1)−N(1)	81.86(6)	79.60(6)
O(1)−Os(1)−N(7)	105.1(9)	101.56(6)
O(2)−Os(1)−N(7)	102.47(8)	105.63(7)
O(1)−Os(1)−O(2)	82.47(7)	84.86(6)

(5) (a) Crevier, T.; Mayer, J. M. *Angew. Chem.* **1998**, *37*, 1891−1892. (b) Crevier, T.; Bennett, B. K.; Soper, J. D.; Bowman, J. A.; Dehestani, A.; Hrovat, D. A.; Lovell, S.; Kaminsky, W.; Mayer, J. M. *J. Am. Chem. Soc.* **2001**, *123*, 1059−1071.

(6) (a) Bennett, B. K.; Pitteri, S.; Pilobello, L.; Lovell, S.; Kaminsky, W.; Mayer, J. M. *J. Chem. Soc., Dalton Trans.* **2001**, 3489−3497. (b) Crevier, T. J. Ph.D. Thesis, University of Washington, 1998. (c) Bennett, B. K.; Saganic, E.; Lovell, S.; Kaminsky, W.; Samual, A.; Mayer, J. M., submitted for publication.

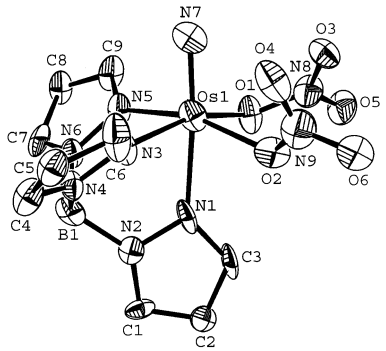

Figure 2. ORTEP drawing of $TpOs(N)(ONO_2)_2$ (**8**).

Table 3. Electrochemical and Spectroscopic Properties of $TpOs(N)X_2$ Complexes

$TpOs(N)X_2$	$E_{p,c}$[a]	$\delta(^{15}N)$[b]	$\nu_{Os\equiv N}$ ($\nu_{Os\equiv ^{15}N}$)[c]	λ_{max} (ϵ)[d]
TFA (**3**)	−1.20	908	1080 (1042)	440 (380)
TCA (**4**)	−1.25	909	1081 (1042)	425 (350)
Br (**6**)	−1.28	887	1068 (1031)	475 (400)
Cl (**1**)	−1.34	890	1066 (1031)	400 (420)
TBA (**5**)	−1.36	907	1082 (1044)	440 (300)
ONO_2 (**8**)	−1.38	922	1059 (1024)	435 (330)
$O_2C_2O_2$ (**7**)	−1.40	884	1070 (1034)	440 (310)
OAc (**2**)	−1.83	881	1087 (1050)	440 (314)

[a] Irreversible Os(VI)/Os(V) peak potentials in V vs $Cp_2Fe^{+/0}$ in MeCN at 0.1 V s^{-1} scan rate. [b] ^{15}N NMR chemical shifts in ppm referenced to $\delta = 0.0$ for aqueous $^{15}NH_4^+$. [c] In cm^{-1}. [d] λ_{max}/nm (ϵ/M^{-1} cm^{-1}) for the visible band; UV bands given in the Experimental Section.

Spectroscopy and Electrochemistry of $TpOs(N)X_2$. ^1H NMR spectra indicate that all of the complexes are diamagnetic and have C_s symmetry, based on the pyrazole peaks of the Tp ligand appearing in 2:1 ratios.[10] ^{15}N-Enriched materials, prepared from $TpOs(^{15}N)Cl_2$,[5] were used to obtain ^{15}N NMR spectra. All the compounds show a single peak between 821 and 922 ppm (Table 3), referenced to external aqueous $^{15}NH_4^+$ ($\delta = 0$). These values are similar to those reported for other nitrido ligands on osmium(VI).[11]

The presence of the nitrido ligand is evidenced by the strong sharp υ(Os≡N) band between 1000 and 1100 cm^{-1} in the IR spectra of **1**−**8** (Table 3).[12] ^{15}N substitution was used to confirm this assignment for each compound because of the many Tp ligand bands in the same spectral region. All $^{14}N/^{15}N$ isotopic shifts agreed well with values calculated from a diatomic harmonic oscillator model. For instance, υ(Os≡N) for **3** and **3**-^{15}N are 1080 and 1042 cm^{-1}, consistent with the calculated shift of 38 cm^{-1}.

UV−vis spectra of the complexes (Table 3) show a broad band in the visible region between 400 and 475 nm ($\epsilon \sim$ 350 M^{-1} cm^{-1}). There are also two intense bands in the UV ($\epsilon > 10^4$ M^{-1} cm^{-1}), at ∼260 and ∼240 nm. In the more symmetrical complexes $Os(N)X_4^-$, Gray, Che, and coworkers have assigned weak absorptions at 400−500 nm to $d_{xy} \rightarrow d_{\pi^*}$ transitions.[13] The d_{π^*} orbitals are the antibonding combination of d_{xz} and d_{yz} with the nitrido p_x and p_y.[13c]

Cyclic voltammograms of **1**−**8** show only irreversible reduction waves, which are attributed to reduction of Os^{VI} to Os^V. The $E_{p,c}$ values vary from −1.20 to −1.83 V vs $Cp_2Fe^{+/0}$. The values are given in Table 3, where the compounds are listed in order of decreasing potentials. In general, the more negative potentials are found for compounds with the more electron donating substituents (acetate and oxalate), and the most easily reduced compound is the trifluoroacetate. While there is a trend within the carboxylate complexes, overall the $E_{p,c}$ values for $TpOs(N)X_2$ do not correlate with any simple parameter for X such as Hammett σ_p parameters, Lever's E_L values,[14] the PL parameters developed by Chatt, Leigh, and Pickett,[15] or the pK_a of HX. We have previously shown that for **1** and a range of related d^2 Tp−osmium and −rhenium complexes, the potentials for oxidation to d^1 species correlate well with Hammett σ_p parameters but the reduction potentials do not.[16]

Reactions with BPh_3 and PPh_3. Compounds **2**−**8** all react with BPh_3 to form borylamido complexes $TpOs[N(BPh_2)Ph]X_2$, as previously reported for **1**.[5] ^1H NMR spectra of the Os(IV) borylamido products closely resemble that of the dichloride derivative. The only exception is the acetate product $TpOs[N(BPh_2)Ph](OAc)_2$ (**9**), which has C_1 rather than C_s symmetry. This is likely due to an interaction between the boron and an acetate oxygen as shown in eq 3.

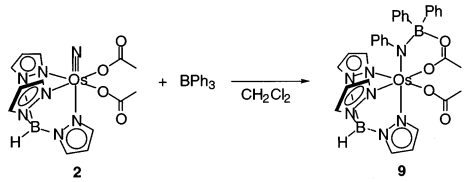

(3)

A similar but apparently weaker B−Cl interaction was found in the structure of $TpOs[N(BPh_2)Ph]Cl_2$.[5] Variable temperature ^1H NMR spectra of the trifluoroacetate derivative **3** showed C_s symmetry down to 213 K. In this case, either a carboxylate interaction analogous to that in eq 3 is not present or it is too weak to give a nonfluxional structure in the NMR.

Competition reactions were used to determine the relative reactivities of the nitrido complexes (Scheme 2). Stock solutions of two osmium complexes in CD_2Cl_2, with C_6Me_6 as an internal standard, were mixed, and a ^1H NMR spectrum

(7) See, for instance: (a) Demadis, K. D.; El-Samanody, E.; Meyer, T. J.; White, P. S. *Polyhedron* **1999**, *18*, 1587−1594. (b) Bright, D.; Ibers, J. A. *Inorg. Chem.* **1969**, *8*, 709. (c) Collison, P. M.; Garner, C. D.; Mabbs, F., E.; Salthouse, J. A.; King, T. J. *J. Chem. Soc., Dalton Trans.* **1981**, 1812−1819. (d) Hunt, S. L.; Shapley, P. A. *Organometallics* **1997**, *16*, 4071−4076. (e) See also refs 8−11.
(8) Nugent, W. A.; Mayer, J. M. *Metal-Ligand Multiple Bonds*; Wiley-Interscience: New York, 1988; Chapter 5.
(9) Chang, P. M.; Yu, W. Y.; Che, C. M.; Cheung, K. K. *J. Chem. Soc., Dalton Trans.* **1998**, 3183.
(10) Abrams, M. J.; Davison, A.; Jones, A. G. *Inorg. Chim. Acta* **1984**, *82*, 125.
(11) Stumme, M.; Preetz, W. *Z. Anorg. Allg. Chem.* **2000**, *626*, 1186−1190.
(12) Griffith, W. P. *J. Am. Chem. Soc.* **1965**, *87*, 3964.
(13) (a) Hopkins, M. D.; Miskowski, V. M.; Gray, H. *J. Am. Chem. Soc.* **1986**, *108*, 6908−6911. (b) Chin, K.-F.; Cheung, K.-K.; Yip, H.-K.; Mak, T. C. M.; Che, C. M. *J. Chem. Soc., Dalton Trans.* **1995**, 657−663. (c) Cowman, C. D.; Trogler, W. C.; Mann, K. R.; Poon, C. K.; Gray, H. B. *Inorg. Chem.* **1976**, *8*, 1747−1751.
(14) Lever, A. B. P. *Inorg. Chem.* **1990**, *29*, 1271−1285.
(15) (a) Butler, G.; Chatt, J.; Leigh, G. J.; Pickett, C. J. *J. Chem. Soc., Dalton Trans.* **1979**, 113. (b) Chatt, J.; Kan, C. T.; Leigh, G. J.; Pickett, C. J.; Stanley, D. R. *J. Chem. Soc., Dalton Trans.* **1980**, 2023. (c) Chatt, J. *Coord. Chem. Rev.* **1982**, *43*, 337.
(16) Bennett, B. K.; Crevier, T. J.; DuMez, D. D.; Matano, Y.; McNeil, W. S.; Mayer, J. M. *J. Organomet. Chem.* **1999**, *591*, 96−103.

Scheme 2

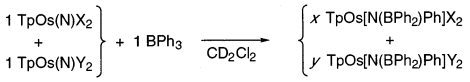

Table 4. Kinetic Results for Reactions of $TpOs(N)X_2$ with BPh_3 and PPh_3

$TpOs(N)X_2$	(k_X/k_{TFA}) for BPh_3	k for BPh_3 (M^{-1} s^{-1})	(k_X/k_{TFA}) for PPh_3
TFA (**3**)	[1]	4100	[1]
TCA (**4**)	0.8	3300	0.95
Br (**6**)	2.1	8600	0.89
Cl (**1**)	1.3	5300	0.85
TBA (**5**)	0.5	2100	0.81
ONO_2 (**8**)	1.3	5200	0.77
$O_2C_2O_2$ (**7**)	1.0	4100	0.75
OAc (**2**)	0.01	41	0.15

was taken to confirm the initial concentrations. Addition of BPh_3 caused an immediate color change from light orange to deep red, consistent with the formation of osmium(IV) amido complexes. Final concentrations were determined by ^1H NMR integration. Each of the 24 different competition experiments was repeated three times, with a reproducibility within 5%. Due to the rapid rates, we were concerned that complete mixing was not obtained prior to reaction. Therefore additional experiments were performed where solid BPh_3 was placed at the top of a tilted NMR tube loaded with the solution containing the osmium complexes, and then the NMR tube was mixed vigorously and quickly. This procedure gave the same results as above within experimental error. The relative rate constants were determined from the initial and final concentrations according to eqs 4 and 5.[17a] As a

$$\ln\left(\frac{[\mathrm{TpOsNX_2}]_f}{[\mathrm{TpOsNX_2}]_i}\right) = \frac{k_x}{k_y}\ln\left(\frac{[\mathrm{TpOsNY_2}]_f}{[\mathrm{TpOsNY_2}]_i}\right) \quad (4)$$

$$\ln\left(\frac{1-[\mathrm{TpOs\{N(Ph)BPh_2\}X_2}]}{[\mathrm{TpOsNX_2}]_i}\right) = \frac{k_x}{k_y}\ln\left(\frac{1-[\mathrm{TpOs\{N(Ph)BPh_2\}Y_2}]}{[\mathrm{TpOsNY_2}]_i}\right) \quad (5)$$

final check, the relative rate constants were found to be transferable. For example, competition reactions between **3** and **1** or **6** gave k_{Cl}/k_{TFA} and k_{Br}/k_{TFA} values of 1.3 and 2.1, whose ratio of 0.62 is consistent with the directly determined k_{Cl}/k_{Br} of 0.65. The relative rates versus $TpOs(N)(TFA)_2$ as the standard complex are given in Table 4.

The kinetics of the reaction between BPh_3 and **2** was examined under second-order conditions in anhydrous CH_2Cl_2 by optical spectroscopy. The absorbance increased throughout the observed spectrum, with the formation of **9** indicated by new peaks at $\lambda_{max} = 270$, 325, 365, and 450 nm. A simple bimolecular rate law (eq 6) is indicated by the reasonably linear integrated rate law (eq 7, Figure 3).[17b] Three independent runs gave $k_{OAc} = 41 \pm 10$ M^{-1} s^{-1} at 25 °C. Using this rate constant and the relative rates from competition experiments, the rate constants for reactions of

(17) Weston, R.; Schwarz, H. *Chemical Kinetics*; Prentice Hall: Upper Saddle River, NJ, 1972; (a) p 16, (b) p 10.

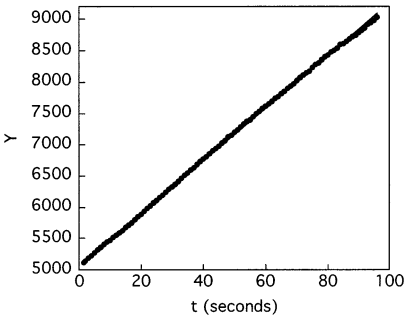

Figure 3. A plot of $Y = \{[\mathbf{2}]_o - [BPh_3]_o\}^{-1} \ln\{[BPh_3]_o[\mathbf{2}]/[BPh_3][\mathbf{2}]_o\}$ vs time for the reaction of $TpOs(N)(OAc)_2$ (**2**) + BPh_3 in CH_2Cl_2 at 25 °C. The reaction is 90% finished by 95 s.

the other osmium complexes with BPh_3 can be calculated (Table 4).

$$\frac{-\mathrm{d}[\mathbf{2}]}{\mathrm{d}t} = k[\mathbf{2}][BPh_3] \quad (6)$$

$$\frac{1}{[\mathbf{2}]_o - [BPh_3]_o}\ln\left(\frac{[BPh_3]_o[\mathbf{2}]}{[BPh_3][\mathbf{2}]_o}\right) = kt \quad (7)$$

Compounds **2**−**8** also react rapidly with PPh_3 to make osmium(IV) phosphiniminato complexes (eq 8). These reactions appear to be very similar to the analogous reaction with **1**, for which the product has been structurally characterized.[6] Competition studies between different $TpOs(N)X_2$ compounds were run in the same manner as BPh_3 described above. The relative rates are given in Table 4.

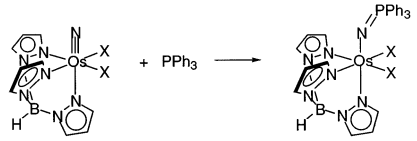

(8)

Discussion

This study compares the spectroscopic, electrochemical, and reactivity properties of a series of osmium nitrido complexes (**1**−**8**). Cyclic voltammetry shows that each compound undergoes an irreversible reduction, and that the peak potentials $E_{p,c}$ vary over a relatively large range of 0.63 V. While irreversible peak potentials are not necessarily related to thermodynamic potentials, the relationship appears to be fairly good in this case. Potentials for the carboxylate complexes, for instance, fall in the order of the pK_a values for the monovalent acids: $O_2CMe \ll$ oxalate $< O_2CCBr_3 < O_2CCCl_3 < O_2CCF_3$. In general, a more electron withdrawing ligand makes the osmium complex more electron deficient and makes $Os^{VI} \rightarrow Os^{V}$ reduction easier. The good correlation of $E_{p,c}$ with rate constant described below further suggests that the $E_{p,c}$ values reflect properties of the $TpOs(N)X_2$ complexes rather than the rates of decomposition of the reduced forms.

A variation of 0.63 V in redox potential corresponds to a change in equilibrium constant for electron transfer of $10^{10.7}$. Given this large difference, the spectroscopic differences between the compounds are quite small. The Os≡N stretching frequencies, ^{15}N NMR chemical shifts, and optical d−d

transition energies vary only slightly over the series. It seems that changes in the X ligands do not change the nature of the bonding and orbital energy gaps, but rather they shift the whole manifold of orbitals up or down. The shifting up of the whole manifold is observed in DFT calculations comparing TpOs(N)Cl$_2$ and the hypothetical TpOs(N)-(CH$_3$)$_2$.[5b] Changing from Cl to Me raises the energy of all orbitals, although not by the same amounts: the nitrido lone pair rises 1.1 eV, the roughly nonbonding d_{xy} HOMO rises 0.7 eV, and the π* LUMOs (d_{xz}, d_{yz}) rise 1.3 eV. The Cl to Me change does affect the HOMO−LUMO gap, from 1.6 to 2.2 eV, in contrast to what is observed for compounds **1**−**8**. This is presumably due to chloride vs methyl being a much larger variation in σ- and π-donor abilities than is found over the whole set of ligands in **1**−**8**.

Electrochemical properties are often assumed to correlate with reactivity. In a series of related molecules, such as **1**−**8**, the derivatives with more favorable potentials for reduction (more positive potentials) should be, in general, more reactive toward reduction by inner-sphere processes such as eqs 2, 3, and 8. Such a connection is intuitively reasonable, but there is no strict thermochemical reason why rates of bond-forming reactions should be related to redox potentials. The connection between one-electron potentials and reactivity is particularly tenuous for the *two-electron* inner-sphere redox processes studied here.

For compounds **1**−**8**, the relative rates of reaction are remarkably insensitive to the reduction potentials. The relative rates for reduction of Os(VI) to Os(IV) by BPh$_3$ vary by only 10^2, and the reactions with PPh$_3$ vary by only a factor of 7. These ranges are very small given that the range of potentials corresponds to $\gtrsim 10^{10}$ in equilibrium constant for electron transfer as noted above. The Brønsted α values for these reactions [the slope of log(k_{rel}) vs log(K_{ET}) plots (taking log(K_{ET}) = $E_{p,c}$/0.059 V)] are 0.2 for BPh$_3$ and 0.08 for PPh$_3$.

The small variation in rate constants for PPh$_3$ + TpOs-(N)X$_2$ correlate quite well with $E_{p,c}$, as shown in the graph of log(k_X/k_{TFA}) vs $E_{p,c}$, Figure 4A. The most easily reduced complex, **3**, reacts the fastest, and the most difficult to reduce, **2**, reacts the slowest. However, relative rate constants for reduction of TpOs(N)X$_2$ by BPh$_3$ do not correlate with $E_{p,c}$, as shown in Figure 4B. The trifluoroacetate complex **3** is more easily reduced than any other complex but reacts more slowly than **1**, **6**, **7**, and **8**. Within the same type of ligand, there appears to be a correlation; for instance, TpOs(N)Br$_2$ is more easily reduced and reacts faster than TpOs(N)Cl$_2$. The relative rates TpOs(N)(TFA)$_2$ > TpOs(N)(TBA)$_2$ > TpOs(N)(TBA)$_2$ > TpOs(N)(OAc)$_2$ follow the electrochemical potentials but only within the acetate series; the oxalate and nitrate complexes do not fit this trend.

The reactions of BPh$_3$ and PPh$_3$ both involve reduction of Os(VI) to Os(IV), but only one correlates with one-electron potentials. This is likely due to differences in the reaction mechanisms. PPh$_3$ addition to nitrido ligands most likely occurs by direct attack of the nucleophilic phosphorus on the nitrogen, at the M−N π* LUMO, as we have suggested for **1**[5b] and as others have proposed in related systems.[18] For instance, Meyer et al. have examined[18c]

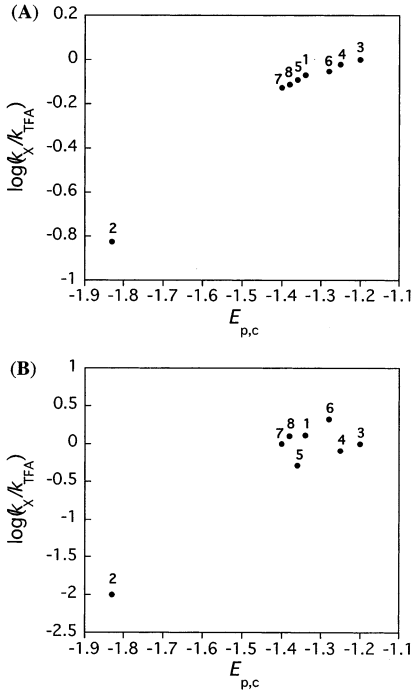

Figure 4. log(k_X/k_{TFA}) vs $E_{p,c}$ for the reactions of TpOs(N)X$_2$ with PPh$_3$ **(A)** and with BPh$_3$ **(B)** (for compound numbers see Table 4).

additions of various phosphines to [(tpy)Os(N)Cl$_2$]$^+$, and Lau et al. have examined how PPh$_3$ addition to the nitrido ligand in Os(N)(L)(Cl) is affected by different substituents on the salen ligand L.[18b] The BPh$_3$ reactions, however, have been found to proceed by a two-step mechanism: initial rapid equilibrium binding of the Lewis-acidic boron to the nitrido lone pair is followed by aryl migration from boron to nitrogen (eq 9).[5b] As previously described, the rate for this process

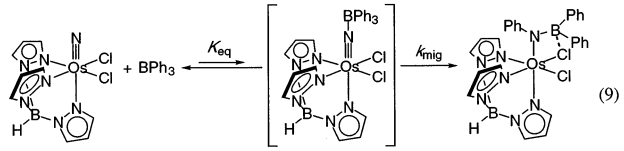

(9)

depends on both K_{eq} and k_{mig} (rate = $K_{eq}k_{mig}$[TpOs(N)X$_2$]-[BPh$_3$]). Aryl groups with higher migratory aptitudes react faster with **1** because of their higher k_{mig}, and more Lewis-acidic boranes react faster because of their higher K_{eq}.[5b] Related nitrido−borane adducts have been reported, including Re(NBPh$_3$)(Et$_2$dtc)$_2$(PMe$_2$Ph)[19] and TpOs[NB(C$_6$F$_5$)$_3$]-Ph$_2$.[5b] The multistep nature of this mechanism means that its rate is unlikely to respond simply to changes in the electrochemical potential of the starting osmium compound. Increased electron density at osmium favors the initial binding but should retard the aryl migration step.

Conclusions

Changing the ancillary ligand X from halide to various carboxylates to nitrate changes the properties of the osmium-

(18) (a) Reference 8, p 245. (b) Wong, T. W.; Lau, T. C.; Wong, W. T. *Inorg. Chem.* **1999**, *38*, 6181−6186. (c) Demadis, K. D.; Bakir, M., Klesczewski, B. G.; Williams, D. S.; White, P. S.; Meyer, T. J. *Inorg. Chim. Acta* **1988**, *270*, 511−526.
(19) Ritter, S.; Abram, U. *Inorg. Chim. Acta* **1995**, *231*, 245.

(VI) nitrido complexes $TpOs(N)X_2$. The irreversible potentials for reduction to Os(V) vary substantially, by 0.63 V, but the IR, ^1H and ^{15}N NMR, and UV−vis spectra are little affected. Thus, the substituents seem to move the whole orbital manifold without strongly affecting the spectroscopic properties of the Os≡N triple bond. The compounds are all reduced to osmium(IV) by PPh_3, to form phosphiniminato complexes $TpOs(NPPh_3)X_2$, and by BPh_3, yielding boryl-anilido complexes $TpOs[N(BPh_2)Ph]X_2$. Similar rate constants are observed for all of the compounds, despite the large range in reduction potential. The insensitivity of the two-electron reactions to one-electron redox potential is noteworthy. The relative rate constants for the PPh_3 reactions correlate well with the cathodic peak potentials, but those for the BPh_3 reactions do not, because of the multistep nature of the mechanism for the latter reactions.

Experimental Section

Materials. All reactions were conducted under air unless stated otherwise. Anhydrous hexane was distilled from Na/benzophenone, while CH_2Cl_2 and CH_3CN were distilled from CaH_2. CD_2Cl_2 and CD_3CN were dried in the same manner and were stored over 4 Å molecular sieves. $TpOs(N)Cl_2$ and $TpOs(^{15}N)Cl_2$ were prepared according to literature procedures.[5b] BPh_3 (Aldrich) was sublimed under static vacuum. Other reagents were purchased from Aldrich and used without further purification.

Instrumentation and Measurements. ^1H NMR spectra were recorded on Bruker AF-300, AM-499, and WM-500 spectrometers at ambient temperatures and referenced to Me_4Si or a residual solvent peak: δ (multiplicity, coupling constant, number of protons, assignment). All pyrazole J_{HH} are 2 Hz. ^{15}N NMR spectra were recorded on a Bruker DMX-750 spectrometer at ambient temperature and referenced using an external aqueous solution of $^{15}NH_4{}^{15}NO_3$. IR spectra were obtained as KBr pellets using a Perkin-Elmer 1600 series FTIR spectrometer at 4 cm^{-1} resolution. Each complex contains a number of stretches associated with the Tp ligands that typically vary less than 3 cm^{-1}: 982 (w), 3112 (m), and 1503 (m), 1075 (m), 657 (m), 615 (m), 1404 (s), 1312 (s), 1216, (s), 1118 (s), 768 (s), 715 (s), and 1046 (vs). Electronic absorption spectra were acquired with a Hewlett-Packard 8453 diode array UV−visible spectrophotometer in anhydrous CH_2Cl_2 and are reported as λ/nm (ϵ/M^{-1} cm^{-1}).

Cyclic voltammograms were measured with a BAS model 100 potentiostat using a three-compartment cell with a $Ag/AgNO_3$ (0.1 M in CH_3CN) reference electrode, platinum disk working electrode, and platinum wire auxiliary electrode. The electrolyte solution was 0.1 M Bu_4NPF_6 (recrystallized from ethanol) in CH_3CN. The solution in the working compartment was deoxygenated and kept under an atmosphere of N_2. Potentials are reported versus internal $Cp_2Fe^{+/0}$. Electrospray ionization mass spectra (ESI/MS) were obtained on a Applied Biosystems Mariner API-TOF mass spectrometer. Samples were introduced in a CH_3CN/H_2O mixture with a nozzle potential set at 140 V. Elemental analyses were performed by Atlantic Microlabs.

$TpOs(N)(OAc)_2$ (2). A 200 mL round-bottom flask was charged with **1** (0.200 g, 0.410 mmol), AgOAc (0.480 g, 2.87 mmol), and 50 mL of acetonitrile. The flask was connected with a condenser and heated with stirring in an 85 °C oil bath for 12 h. The solution was cooled to room temperature, filtered to remove AgOAc and AgCl, and reduced to 5 mL. Chromatography on silica gel with CH_2Cl_2/acetone (95/5) as the eluant gave an orange band, which was stripped to dryness, yielding orange **2** (0.190 g, 0.355 mmol, 87%). ^1H NMR (CD_2Cl_2): 6.16 (t), 7.57 (d), 7.58 (d) (each 1H, pz); 6.44 (t), 7.85 (d), 8.21 (d) (each 2H, pz); 2.23 (s) (6H, CH_3). ES/MS: 538 (M^+). IR: 1087 cm^{-1} (νOs≡^{14}N); νOs≡^{15}N, 1050 cm^{-1} (calculated 1051 cm^{-1}). UV/vis: 440 (314), 260 (7500), 230 (11000). Anal. Found: C, 29.35; H, 3.07; N, 18.20. Calcd for $C_{13}H_{16}BN_7O_4Os$: C, 29.17; H, 3.01; N, 18.32.

$TpOs(N)(TFA)_2$ (3). A solution of trifluoroacetic acid (144 μL, 1.87 mmol, 10 equiv) and **2** (0.100 g, 0.187 mmol) in 10 mL of acetone was stirred for 1 h in air. The solvent solution was removed in vacuo and the residue redissolved in 2 mL of CH_2Cl_2 and chromatographed (silica gel, CH_2Cl_2/hexane (80/20) as the eluant). An orange band was collected, and orange **3** (0.09 g, 0.140 mmol, 74% yield) was obtained by vapor diffusion of hexane into a CH_2Cl_2 solution. ^1H NMR (CD_2Cl_2): 6.20 (t), 7.52 (d), 7.64 (d) (each 1H, pz); 6.54 (t), 7.95 (d), 8.15 (d) (each 2H, pz). ES/MS: 645 (M^+). IR: 1081 cm^{-1} (νOs≡^{14}N); νOs≡^{15}N, 1042 cm^{-1} (calculated 1044 cm^{-1}). UV/vis: 440 (265), 260 (7500), 230 (11000). Anal. Found: C, 24.19; H, 1.47; N, 15.10. Calcd for $C_{13}H_{10}BF_6N_7O_4Os$: C, 24.27; H, 1.57; N, 15.24.

Preparations of 4−10 all followed the procedure described above for **3** using different acids. **$TpOs(N)(TCA)_2$ (4).** Yield = 75%. ^1H NMR (CD_2Cl_2): 6.17 (t), 7.63 (d), 7.68 (d) (each 1H, pz); 6.55 (t), 7.95 (d), 8.20 (d) (each 2H, pz). ES/MS: 744 (M^+). IR: 1080 cm^{-1} (νOs≡^{14}N); νOs≡^{15}N, 1042 cm^{-1} (calcd 1043 cm^{-1}). UV/vis: 425 (350), 260 (8400), 230 (12000). Anal. Found: C, 21.20; H, 1.45; N, 13.12. Calcd for $C_{13}H_{10}BCl_6N_7O_4Os$: C, 21.04; H, 1.36; N, 13.21. **$TpOs(N)(TBA)_2$ (5).** Yield = 63%. ^1H NMR (CD_2Cl_2): 6.19 (t), 7.63 (d), 7.83 (d) (each 1H, pz); 6.54 (t), 7.95 (d), 8.21 (d) (each 2H, pz). ES/MS: 1010 (M^+). IR: 1082 cm^{-1} (νOs≡^{14}N); νOs≡^{15}N, 1045 cm^{-1} (calcd 1044 cm^{-1}). UV/vis: 440 (300), 260 (11000), 230 (19000). Anal. Found: C, 15.53; H, 1.00; N, 9.52. Calcd for $C_{13}H_{10}BBr_6N_7O_4Os$: C, 15.48; H, 1.07; N, 9.72. **$TpOs(N)Br_2$ (6).** Yield = 62%. ^1H NMR (CD_2Cl_2): 6.03 (t), 7.47 (d), 7.52 (d) (each 1H, pz); 6.55 (t), 7.91 (d), 8.46 (d) (each 2H, pz). ES/MS: 1010 (M^+). IR: 1068 cm^{-1} (νOs≡^{14}N); νOs≡^{15}N, 1032 cm^{-1} (calcd 1031 cm^{-1}). UV/vis: 475 (400), 260 (10000), 240 (13000). Anal. Found: C, 19.00; H, 1.89; N, 16.67. Calcd for $C_9H_{10}BBr_2N_7Os$: C, 18.73; H, 1.75; N, 16.99. **$TpOs(N)(O_2C_2O_2)$ (7).** Yield = 63%. ^1H NMR (CD_2Cl_2): 6.19 (t), 7.63 (d), 7.83 (d) (each 1H, pz); 6.54 (t), 7.95 (d), 8.21 (d) (each 2H, pz). ES/MS: 1010 (M^+). IR: 1070 cm^{-1} (νOs≡^{14}N); νOs≡^{15}N, 1034 cm^{-1} (calcd 1033 cm^{-1}). In the preparation of **7**, the solution was heated at 50 °C for 1 h to speed up the rate. UV/vis: 440 (310), 260 (8000), 230 (11000). Anal. Found: C, 26.03; H, 1.86; N, 19.33. Calcd for $C_{11}H_{10}BN_7O_4Os$: C, 26.15; H, 1.99; N, 19.41. **$TpOs(N)(ONO_2)_2$ (8).** Yield = 42%. ^1H NMR (CD_2Cl_2): 6.19 (t), 7.63 (d), 7.83 (d) (each 1H, pz); 6.54 (t), 7.95 (d), 8.21 (d) (each 2H, pz). ES/MS: 1010 (M^+). IR: 1059 cm^{-1} (νOs≡^{14}N); νOs≡^{15}N, 1024 cm^{-1} (calcd 1023 cm^{-1}). UV/vis: 435 (330), 260 (10000), 230 (12000). Anal. Found: C, 19.79; H, 1.70; N, 23.20. Calcd for $C_9H_{10}BN_9O_6Os$: C, 19.97; H, 1.86; N, 23.29.

$TpOs\{N(Ph)BPh_2\}(OAc)_2$ (9). A solution of **2** (0.100 g, 0.205 mmol), BPh_3 (49 mg, 0.205 mmol), and 20 mL of CH_2Cl_2 was stirred for 10 min and then run down a column of silica gel with 70/30 CH_2Cl_2/hexane, yielding **9** as a dark orange solid (0.139 g, 0.178 mmol, 87%). ^1H NMR (CD_2Cl_2): 5.92 (1H, t, pz), 6.00 (1H, t, pz′), 6.39 (1H, t, pz″), 6.07, 6.52 (each 1H, d, pz), 5.50, 7.14 (each 1H, d, pz′), 7.41, 7.53 (each 1H, d, pz″); 4.92 (d, 7 Hz, 2H, NPh_o), 7.02 (t, 7 Hz, 2H, NPh_m), 6.61 (t, 7 Hz, 1H, NPh_p), (d, 7 Hz, 4H, BPh_{2ortho}), (d, 7 Hz, 4H, BPh_{2meta}), (d, 7 Hz, 2H, BPh_{2para}); 3.28 (s, 3H, CH_3), 2.05 (s, 3H, CH_3). ES/MS: 780 (M^+). UV/vis: 450 (5700), 365 (6100), 325 (8100), 270 (13700). Anal. Found:

C, 47.52; H, 4.76; N, 11.95. Calcd for $C_{29}H_{31}B_2N_7O_4Os \cdot C_3H_6O$: C, 47.36; H, 4.60; N, 12.08 (1 mol of acetone is observed in ^{1}H NMR spectra after recrystallization).

Competition Studies. All manipulations were done in a glovebox with anhydrous CD_2Cl_2. In a typical procedure, four 2 mL volumetric flasks were charged with **3** (7 mg, 11 μmol,), **4** (8 mg, 11 μmol), BPh_3 (11 mg, 45 μmol), and C_6Me_6 (40 mg, 0.247 mmol), respectively. The volumetric flasks containing C_6Me_6 and BPh_3 were each taken up with 2 mL of CD_2Cl_2. The C_6Me_6 solution (50 μL, 6 μmol) was added to the flasks with **3** and **4**, and each was taken up to 2 mL with CD_2Cl_2, giving solutions 3.1 mM in C_6Me_6 and 5.5 mM in **3** or **4**. Three separate sealable NMR tubes were charged with (i) 0.350 mL of the solution of **3**, (ii) 0.350 mL of the solution of **4**, and (iii) 0.175 mL of each of the solutions of **3** and **4**. ^{1}H NMR spectra were taken, and the tubes were returned to the glovebox. One equivalent of BPh_3 (86 μL) was added to tubes i and ii. BPh_3 (0.5 equiv, 43 μL) was added to tube iii, tilting the NMR tube sideways to make sure none of the BPh_3 solution touched the osmium solutions. The NMR tubes were then mixed vigorously and quickly. Integration of the NMR spectra gave the product yields.

Kinetic Studies. All manipulations were done in a glovebox. Two separate 25 mL volumetric flasks were charged with **2** (23 mg, 43 μmol) and BPh_3 (11 mg, 45 μmol) and brought up to 25 mL with CH_2Cl_2 (1.7 mM **2**, 1.8 mM BPh_3). A quartz UV cell was charged with the solution of **2** (1.5 mL, 0.0025 mmol) and covered with a septum. The BPh_3 solution (1.5 mL, 0.0027 mmol) was added to the cuvette by gastight syringe, the solution was mixed, and absorption spectra were taken every second for 5 min. The solution was removed in vacuo and taken up in anhydrous CD_2Cl_2, and a NMR spectrum was taken to confirm the formation of **9**, the complete depletion of **2**, and the small excess of BPh_3.

Crystal Structures of 3 and 8. Both crystals were grown by slow evaporation of hexane/methylene chloride solutions. Crystals were mounted on a glass fiber with epoxy. Data were collected on a Nonius KappaCCD diffractometer. Data for **3** was collected at 20 °C by rotation about the ϕ axis in 0.8° increments over 129.9°. **8** was cooled to −143 °C, and then the data was collected by rotation about the ϕ axis in 1° increments over 179.9°. The exposure times per frame and the crystal−detector distances were 40 s and 30 mm for both **3** and **8**. The merging *R* factors of 0.0933 (**3**) and 0.1701 (**8**) indicated that the data were not of good quality. Solutions by direct methods produced a complete phasing model for **3** and **8** with the rest located by difference Fourier synthesis. All heavy atoms were refined anisotropically by full-matrix least-squares. All hydrogen atoms were located using a riding model.

Acknowledgment. We are grateful to Dr. Nancy Doherty (University of California at Irvine) for helpful discussion on ^{15}N NMR. We thank Dr. Ross Lawrence for mass spectrometry, and Dr. Joanna Long for ^{15}N NMR experiments. We are grateful to the National Science Foundation for financial support. We thank Dr. Tom Crevier and Tara Conrad for initial studies on $TpOs(N)(OAc)_2$.

Supporting Information Available: Complete crystallographic data (CIF) for complexes **3** and **8**. This material is available via the Internet at http://pubs.acs.org.

IC0260264